[1] **Shivam Singh**

[2] **Satyam Kumar Upadhyay**

Improvement of Power Factor in Wireless Electric Vehicle Charging Using Inductive Power Transfer Topology

Journal of Electrical Systems

Abstract: - The EV requires energy supplied to its motors to function properly. This required energy either can be transmitted by a physical wired connection or by wireless power transfer firstly to the battery using charging of the EV system and then battery discharges to supply to the vehicle. This paper deals with the wireless transfer of power using the induction method for charging battery of the vehicle using electric energy for its functioning as it is the most suitable and fast mode to charge the batteries of many vehicles altogether at charging station. The challenges recently faced by EV's includes the movement of energy from the energy supply point to the destination i.e., EV's without the direct interaction of battery and energy source. Many topologies have been introduced in this regard and several simulation models are built.

Keywords: Inductive Power Transfer (IPT), Electric Vehicles (EV), Power Factor (PF), Battery, Wireless Energy Transfer (WET), etc.

I. INTRODUCTION

The global increase in users of vehicles and unavailability or reduction of power sources is a major concern. Alternative to regular fuel-based vehicles is the use of electric vehicles. The EV uses a battery, which gives them the power of operation. Battery charging through various ways and different topologies one of which is Wireless energy transfer (WET), the most recent technological advancement achieved after years of dedicated hard work by various researchers. WET is used for implementation in many domains like battery charging of EV's, battery charging of mobile phones, remotes, etc. The batteries are used to provide energy during the discharging period of operation. It is therefore tried to achieve that at every place where a battery is used to provide the supply of power, the charging of that battery is should be done through the wireless medium. This will decrease the use of clumsy wires and also the losses which occur during the wired transfer of power. One of the many proposed topologies includes ZVZCS topology, which abolished the requirement of the processor having extremely high power thus increasing the efficiency up to 9.26% and reducing the price of establishing a system, based on it [1]. In this paper, the authors have also tried to implement a similar topology to attain a better power factor and a lower percentage of total harmonic distortion. Also, the proposed system provides the least ripples of voltage and current when input is given and output is received by the system.

The induction method used for the charging of the battery of e-vehicle using wireless transmission pictorially is shown through a basic diagram in figure 1.

Fig. 1. Wireless EV charging using the Induction method

[1] M.tech Department of Electrical Engineering Unsiet, VBS Purvanchal University Jaunpur. shivamaa181997@gmail.com

[2] Assistant Prof., Department of Electrical Engineering Unsiet, VBS Purvanchal University Jaunpur. ersatyam126@gmail.com

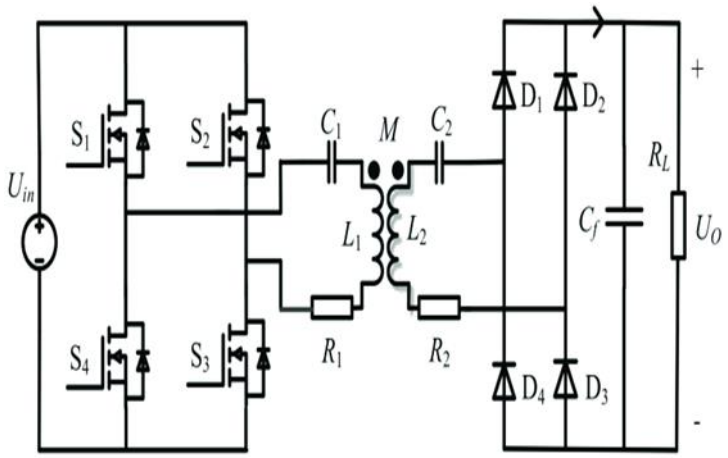

Fig. 2. Structure of Inductive power transfer topology for an EV [2]

II. LITERATURE REVIEW

DC-DC converters are preferable as they have the capacity of soft-switching along with the bidirectional converter if required [2]. Figure 2 shows the off-board side of transmission from the utility grid and the on board reception side of the load, which, in our case is the battery and the vehicle [3].

The e-vehicle is supplied the power from the battery. The transfer of such power from single/three phase supply of AC through AC/DC PFC, then DC to AC containing high frequency to primary compensation thus transferring the energy supply to transmitting coil is in the primary side of figure 3. The secondary side of figure 3 shows the receiving coil, which is connected to the secondary compensation AC/DC conversion to provide energy to the battery for charging.

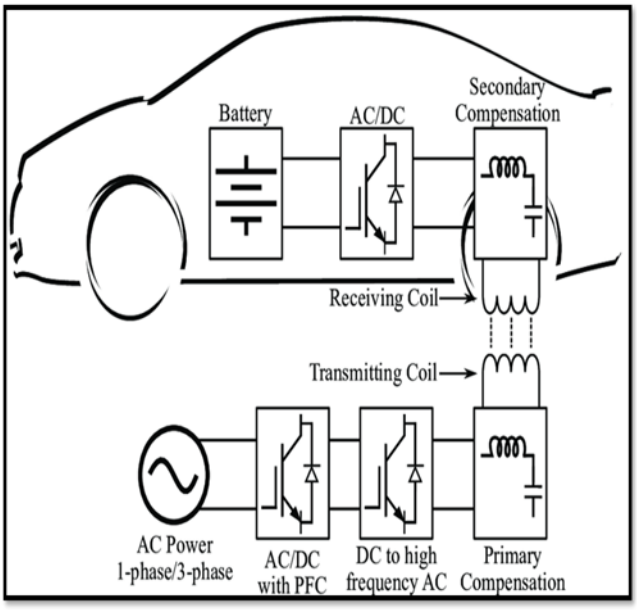

Fig. 3. Inductive power transfer from EV charger to the vehicle [4]

The use of the high-power factor is required for large-scale implementation because it enhances the charging and control of the EV system [4]. The use of resonant WET for charging has considerably changed future scenarios as the key goal is to achieve higher efficiency while charging the system [5]. Seventy percent of the magnetic volume is decreased using D magnetic coupler with the help of BAB converter. Thus, current is bifurcated using double DC inductor [6]. A virtual inertia controller for inductive charging allows the transfer of energy from the grid to the EV by regulating the frequency change of the grid and adjusting the switching cycles accordingly [7]. Design of the coil for optimized energy transfer is achieved using finite element analysis for better performance in interoperability and efficiency of the overall power transfer system [8]. A hybrid IPT system maintains an almost unity power factor to avoid sophistication during the control process at zero phase angle [9]. The state of charge the

of battery is highly influenced by the variation in rated and real temperature of the battery because of the deviation in the demand of the auxiliary power and decrease in the capacity because of the increased exposure of the battery to the high temperature [10]. Figure 4 shows the series–series compensation using the IET for the EV charging during the grid-connected mode of operation.

IPT system equations using KVL and KCL are given by equation 1 to equation 4 [11]

$$Vin - rpIp - LppIp - Vcp + Lm\,pIs = 0 \quad (1)$$

$$LmpIp - Vcs - LspIs - rsIs - VoSgn\,(Is) = 0 \quad (2)$$

$$Cpp\,Vcp = Ip \quad (3)$$

$$Csp\,Vcs = Is \quad (4)$$

Where, Ip is current in the primary coil, Is is current in the secondary coil, Vin is the voltage of the input side and Vo is the output voltage on the secondary side. Current passing through the inductor on the secondary side is given by equation 15 and the coupling factor is given by equation 16

$$Iqds = ZmVs/ZssZpp - Z2m \quad (5)$$

$$K = Lm/(LpLs)^{½} \quad (6)$$

where Zpp = rp + jωeLp + 1/jωeCp , Zss = rs + jωeLs + 1 jωeCs + R, Zm = jωeLm, Vs = − j4Vm/π , R = 8Vo π^2Io

This allows the efficient zero voltage switching at the resonant frequency of the operating system leading to the reduction of inductance on the secondary side. The technique used for achieving such a system is called the harmonic balance technique, which finds the steady state system and transient system of the coil [11]

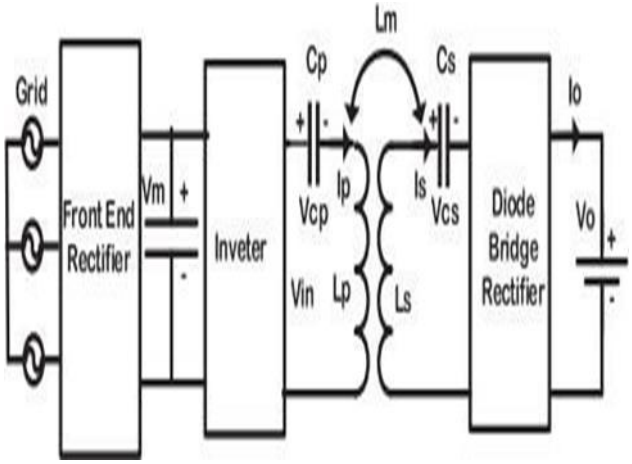

Fig. 4. Series compensation of inductive energy transfer [5]

Figure 5 shows the circuit diagram of the converter used for power transfer using the induction topology. The transfer of power occurs in eight modes

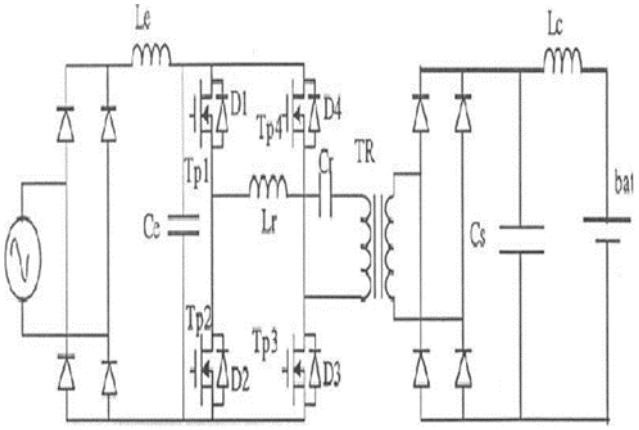

Fig. 5. Circuit Diagram of the power transfer through the induction process [6]

For wireless grid integration of EV, bidirectional energy transfer using inductive topology has been developed in recent times, which improves the spatial tolerance and performance of the system. With the constant duty cycle and

proper synchronization, double full-bridge converters are used to operate the magnetic couplers. Alternative to BD-IET
is (BAB) boost active bridge type converter replacing the conventional converters, as they don't need the extra switching device when variation in the loading conditions are frequent.

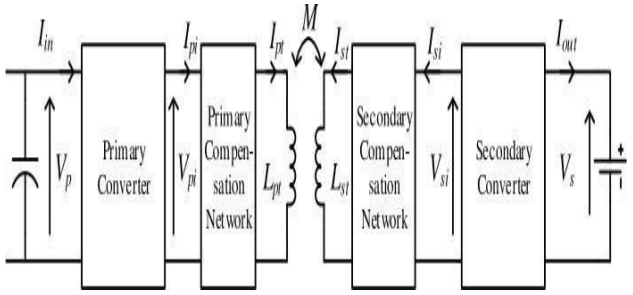

Fig. 5. Block diagram of BD-IET system for vehicle to grid application [7]

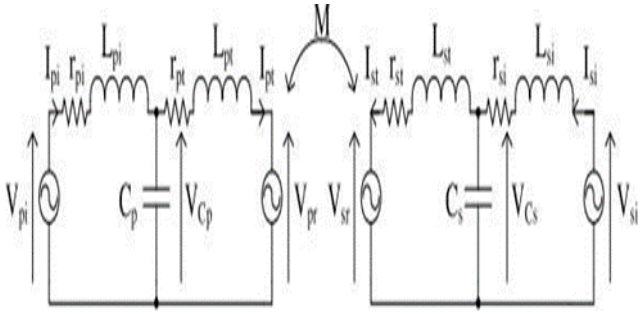

Fig. 6. Phasor domain representation of the BD-IET system. [8]

Figure 5 shows the bi-directional wireless power transfer i.e., BD-IET system for V2G applications and figure 6 shows the phasor domain representation of the BD- IET system using LCL networks. [12]. Volume of the system is reduced by the use of one receiver coil which regulates the output voltage of series connected (SARCs) semi-active rectifier cells. Full tuning condition is achieved by the addition of inductor leading to additional reactance on the receiver side. Reactive power losses are minimized with the help of this topology as it help to attain a unity power factor and switching at zero voltage. Figure 7 shows the multiple output SARC based IET system structure [13].

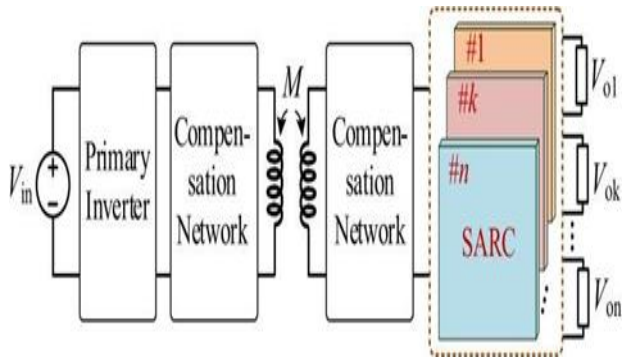

Fig. 7. Structure of IET system output using SARC [9]

Figure 8(a) shows the variable inductor connected with IET system on transmission side and figure 8 (b) shows the double E core used in the variable inductor and the biased DC current [13]. Another application of WET is transfer of energy to UAV (Unmanned Aerial Vehicles). The charging efficiency is improved for UAV by using hybrid control method for regulating output voltage by implementing the PFC boost converter thus providing a DC-link control [14]. By redesigning the coupling coefficients and frequency splitting, underwater WET is also possible [15-18].

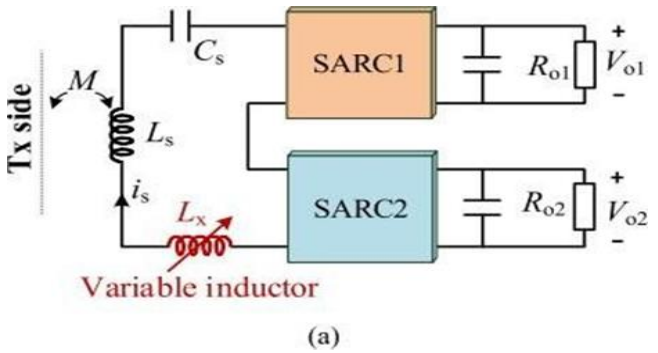

(a)

Fig. 8. (a) Circuit diagram of IET system with inductor [10]

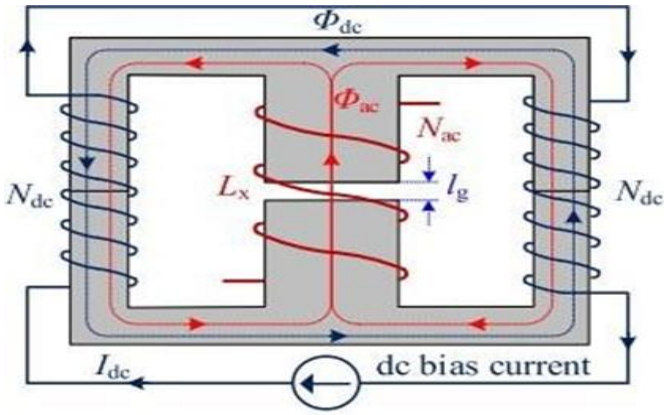

(b)

Fig. 8. (b) Circuit diagram of IET system using double E core and biased DC current [11]

III. PROPOSED METHODOLOGY

Nowadays, the use of electric vehicles is growing quickly. Such a vehicle's efficient charging is a very complicated process. The provision of adequate electricity quality is the main challenge. We employed certain techniques in the suggested system to improve the power quality. The complicated circuit of the wireless charging uses a high-frequency dc-to-ac converter to provide HF ac output. One of the primary goals of this system is to develop an effective wireless charging system employing various DC-DC converters. The purpose of a dc-dc converter is to raise the source voltage's pf. The source power is impacted by the dc load when the ac system is coupled to a dc load via a rectifier. If more AC loads are introduced to this system. Then other loads receive the low pf. So, in the suggested method, we employ a boost and a cuk converter to enhance the pf. We compare the outcomes of both converters with regard to pf correction. The proposed system's simulink graphic shows a dc- dc converter and a dc-ac converter.

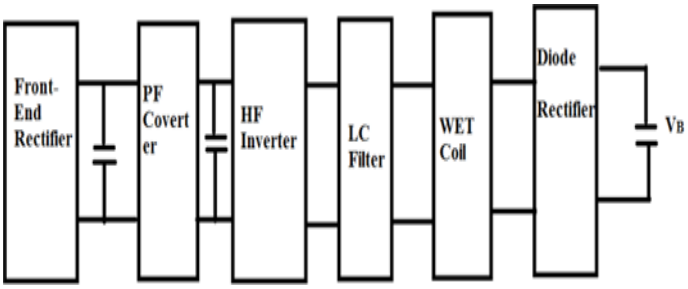

Fig. 9. Block Diagram of Proposed System [5]

IV. MATLAB/SIMULINK MODEL

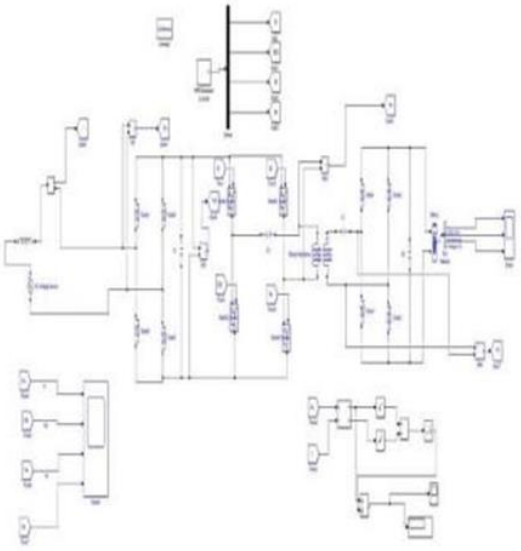

Fig. 10. Final stage of IPT EV charger MATLAB/Simulink model

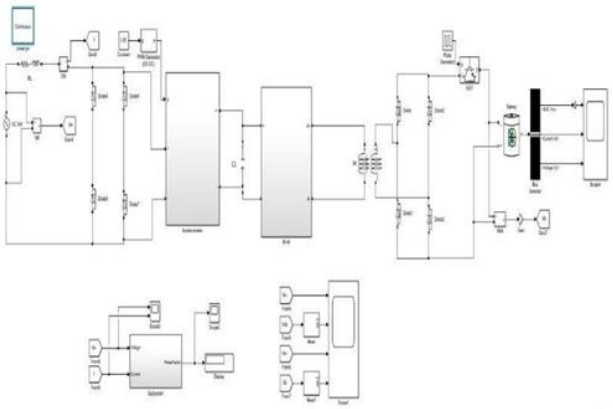

Fig.11. Final stage of IPT EV charger MATLAB/Simulink model

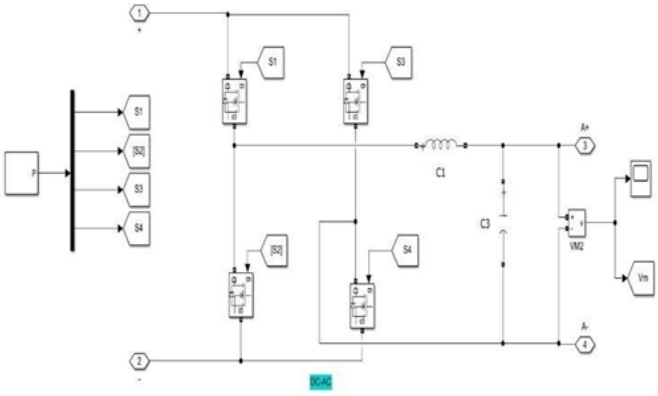

Fig. 12. DC to AC conversion MATLAB/Simulink model

Figure 12 shows the Simulink model of the conversion subsystem from DC to AC

V. RESULTS AND DISCUSSION

This section's findings come from a model sans power factor controller. Figure 13 shows the input ac voltage for the proposed system. The value of the source voltage is 600 volts. Figure 14 displays the results of contribution energy rectification. The direct current power seen in the picture is then obtained. The outcomes of high frequency

voltage conversion utilizing a dc-ac converter are shown in Figure 15. High frequency makes it difficult to see the waveform properly. Figure 16 depicts the zoom portion of the HF output voltage.

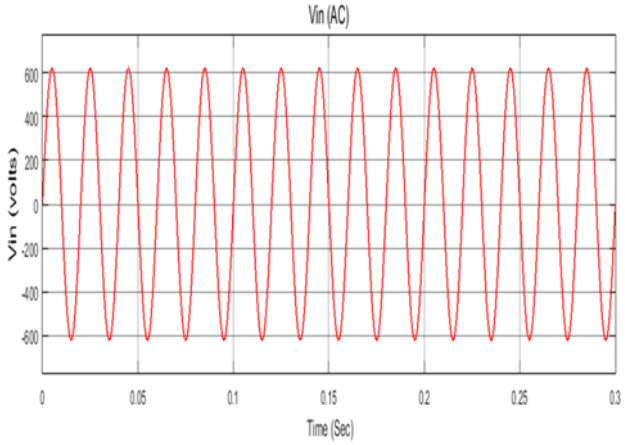

Fig. 13. Input AC voltage waveform

Figure 13 above depicts the source voltage waveform. The input voltage for the proposed system is 600 AC

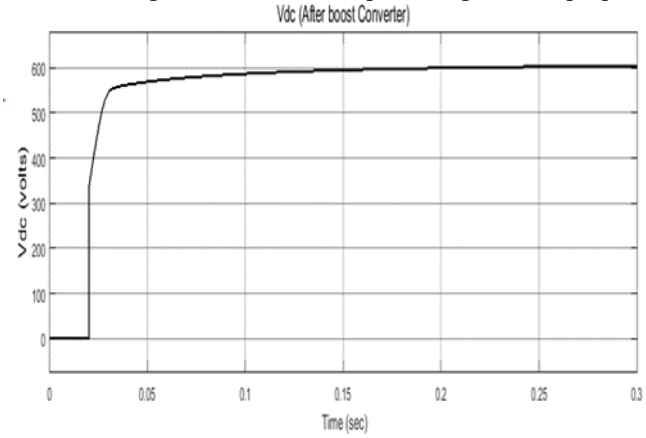

Fig. 14. boost converter o/p

The boost converter output voltage is shown in Figure 14. The above figure clearly depicts 600 volts DC. To turn it into AC, it is further applied to an inverter.

The induction approach is used to transmit the HF inverter's output to the battery. The state of charge value increases over time as the battery charges, as seen in figure 18. It follows that charging starts as soon as the battery is connected to the specified system. As seen in figure 17, 220 volts is applied across the battery.

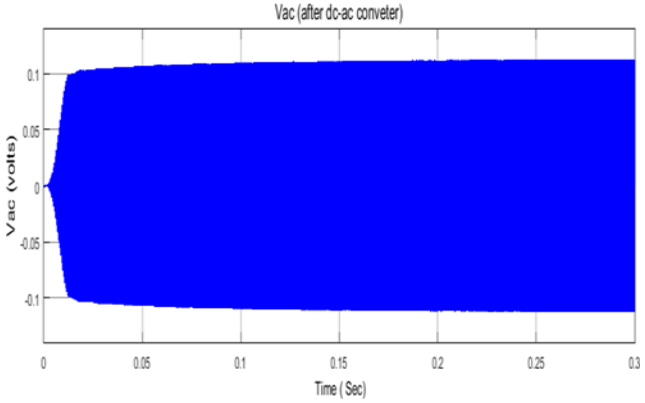

Fig. 15 DC-AC converter o/p

Due to this unclear figure 15, an HF inverter uses high frequency conversion to convert DC to AC. It is evident in figure 16 below. It allowed us to clearly discern a sinusoidal AC signal.

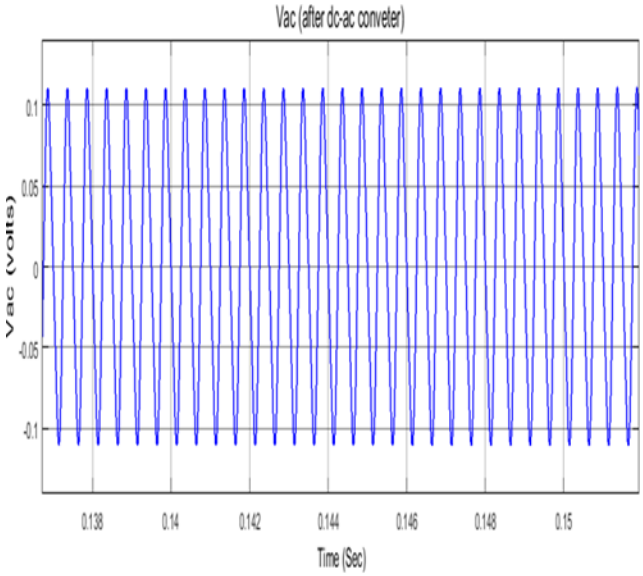

Fig. 16 DC-AC converter o/p

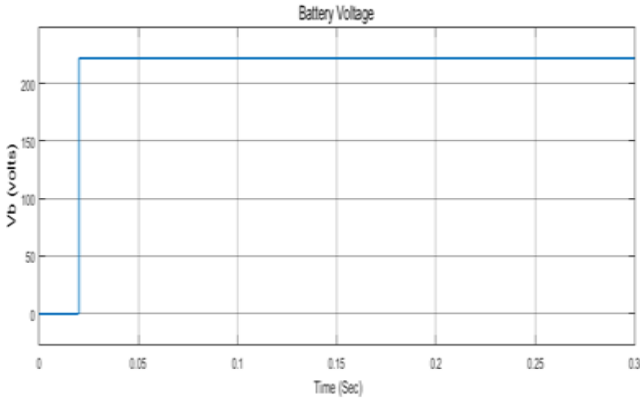

Fig.17. DC-AC converter o/p

Figure 17 above clearly illustrates the 220 volts at which the battery is operating. Because the battery is linked inside the car, the voltage at the battery end should remain consistent throughout time

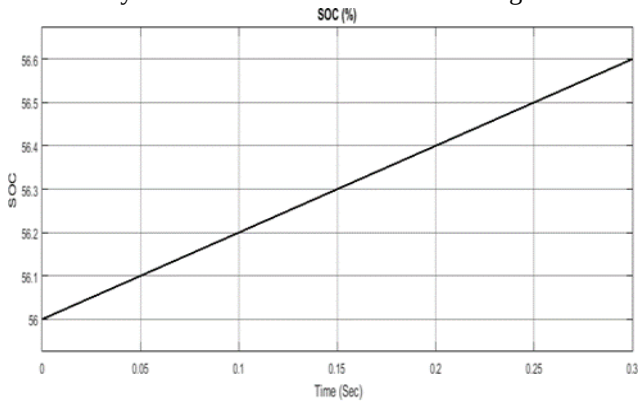

Fig.18. Battery SOC

The battery's SOC is rising. It denotes the battery is in the charging mode

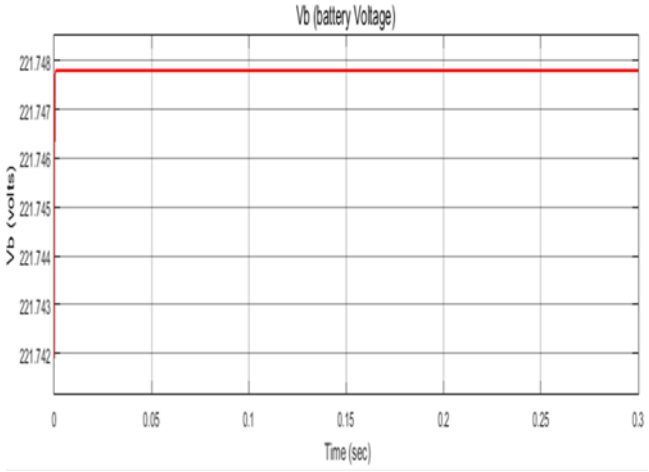

Fig. 19. Battery Voltage

Figures 19 and 20 above show the battery's voltage and current. The voltage is close to 220 volts dc and the current is negative since the battery is charging. Pf in this model is close to 0.7. Figure 21 shows is unhealthy for the system. System harmonics are fairly strong and Pf is quite low.

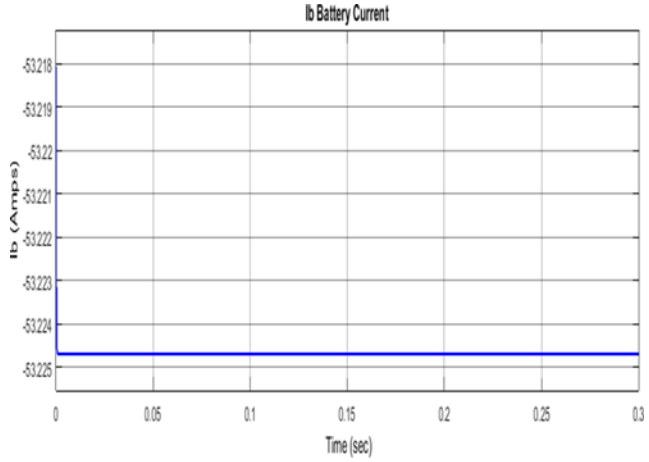

Fig. 20 Battery Current

The power factor value is displayed in figure 21 above without the use of a pf controller. The value is 0.8544 and is low; two distinct ways are being employed in the system, and the outcomes are being demonstrated further. Power quality in the system is also higher if pf is higher. Therefore, some converter is employed in the suggested system to enhance the harmonics and pf, and the results are shown in more detail

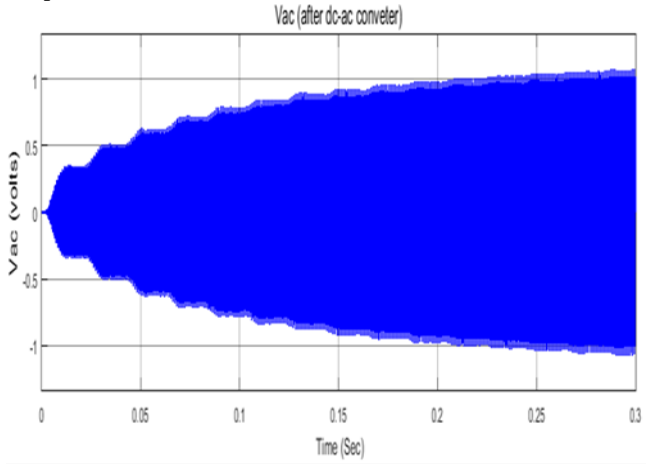

Fig. 21 HF inverter o/p

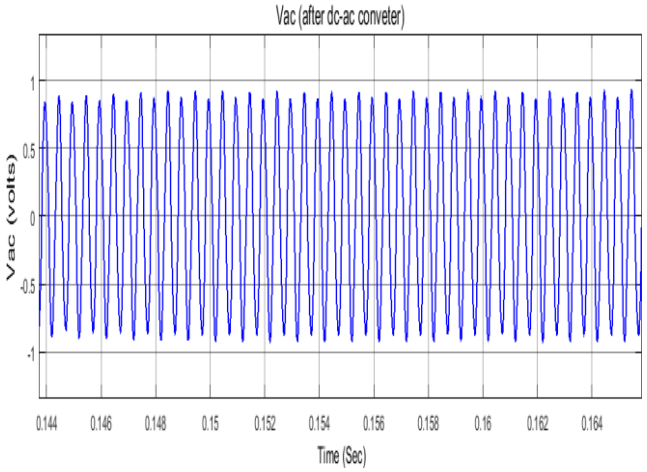

Fig. 22. Zoom HF inverter o/p

The outcomes of the hf inverter ac voltage and cuk boost dc voltage are depicted in the aforementioned figures 21 and 22, respectively. As mentioned before, this model's input is likewise 600 volts.
The zoom portion of the inverter output is shown in the figure22 . This figure is greater than the previously described value without the model.

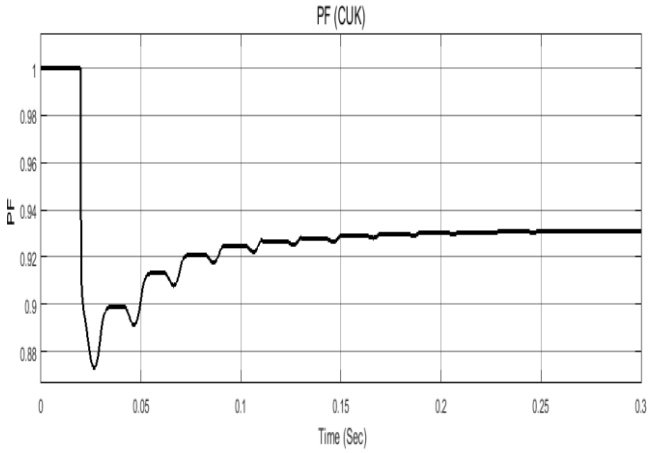

Fig. 23. PF in CUK Model

The inverter output voltage is displayed in this section. The simulation runs for 0.3 seconds, but the inverter's output frequency is quite high—roughly 2 kHz—so this zoom portion displays the output inverter voltage in sinusoidal form. Pf has a value of 0.912, as seen in figure 23.

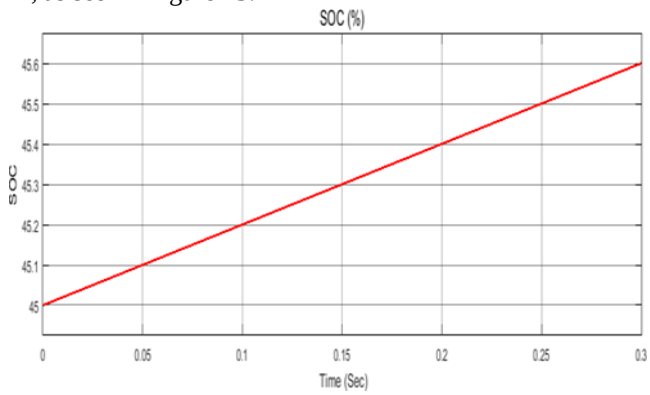

Fig. 24. Battery SOC in CUK Model

The value of the battery's charging status, which is growing, is shown in figure 26 above

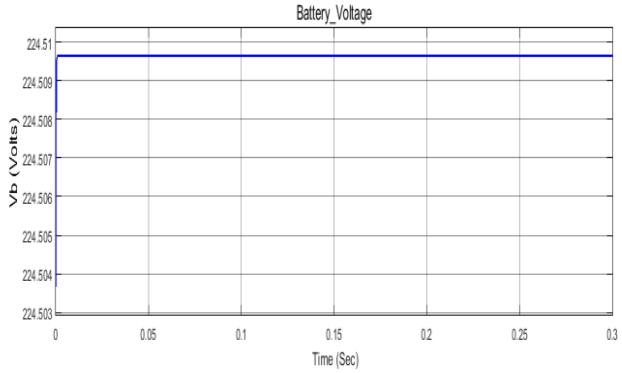

Fig.25. Battery Voltage in CUK Model

When SOC rises above 45 percent, it indicates that the car battery is charging. Figure 27 depicts the voltage across the battery, which remains constant during the charging model.

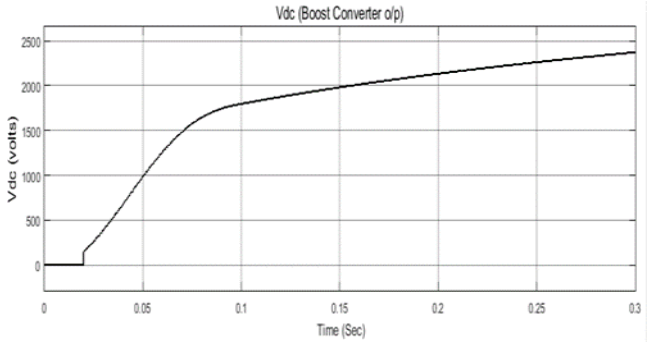

Fig.26. Boost o/p voltage

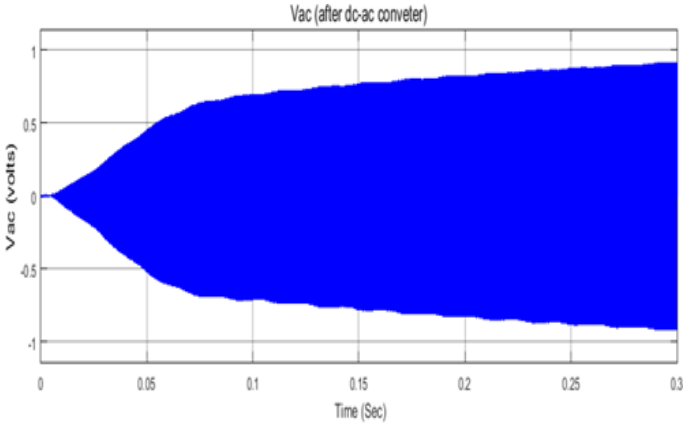

Fig. 27. Boost inverter o/p voltage

Results based on the Boost converter are shown and discussed in this section. We achieve better outcomes than with earlier methods.

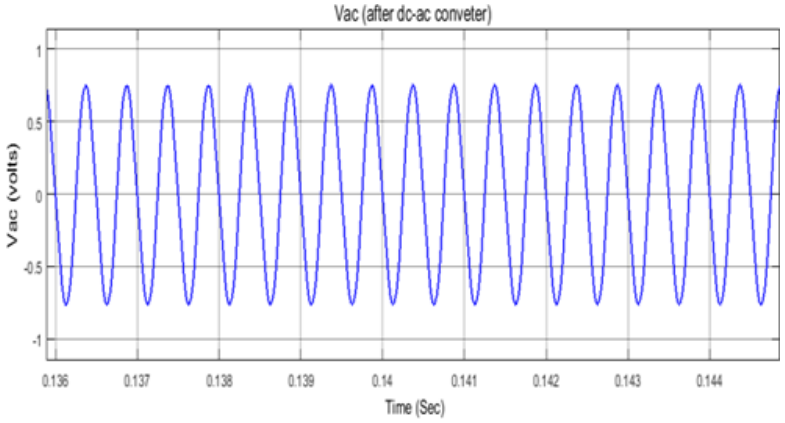

Fig. 28. Zoom Boost inverter o/p voltage

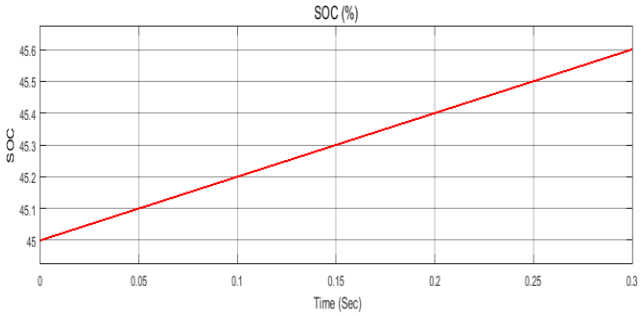

Fig. 29. SOC of Boost Model

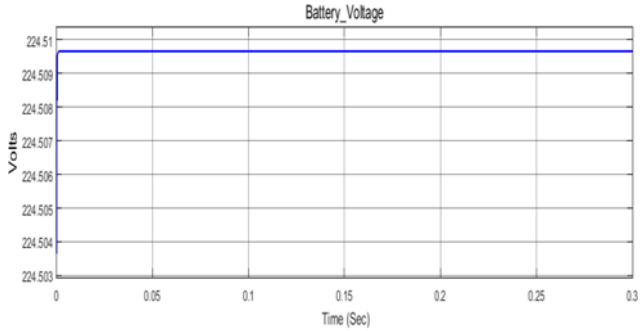

Fig. 30. Vb Battery Voltage of Boost Model

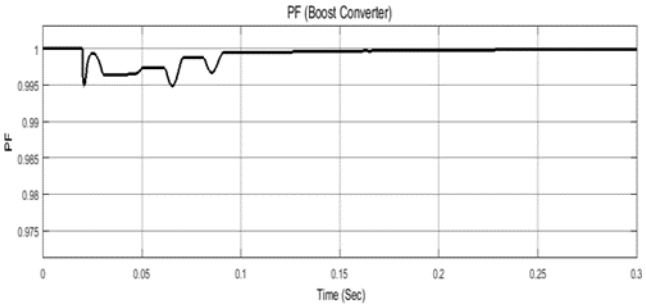

Fig. 31. PF boost Converter

The boost converter output voltage is shown in figure 32 above. The output voltage of the boost converter is further linked to the inverter. Figure 5.20 depicts the inverter output, and Figure 33 depicts the zoom component of this. Figure 33 depicts the battery charging status and is growing. Since SOC is growing, the battery is charging for starting states ranging from 45 to higher values.

The boost converter output voltage is shown in figure 5.19 above. The output voltage of the boost converter is further linked to the inverter. Figure 31 depicts the inverter output, and Figure 32 depicts the zoom component of

this. Figure 33 depicts the battery charging status and is growing. Since SOC is growing, the battery is charging for starting states ranging from 45 to higher values.

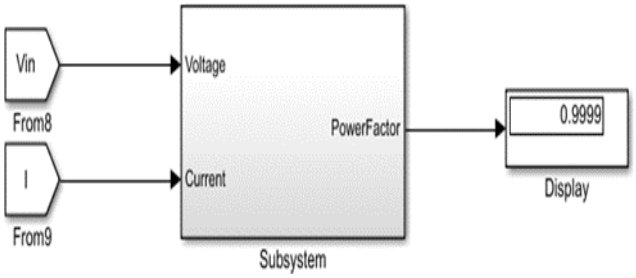

Fig. 32. PF value in Boost Model

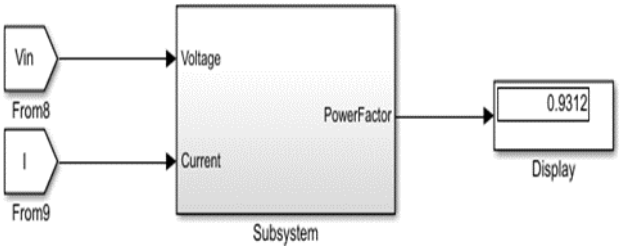

Fig. 33. PF in CUK Model

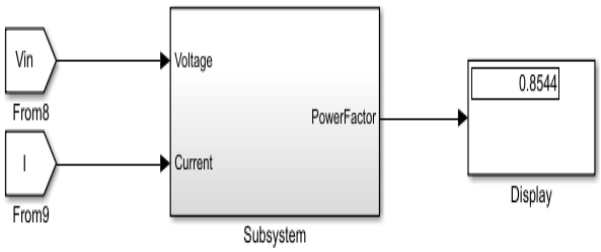

Fig. 34. Pf in Without Pf controller

Here in the above figure, it has been mentioned that the power factor for boost model is noted to be 0.9999, for cuk model is noted to be 0.9312 and for pf in without pf controller is noted to be 0.8544. The pf is good for boost model.

VI. CONCLUSION

Here in the manuscript, we have successfully developed the Simulink/MATLAB model of a wireless battery charging system using the topology of transfer of power through the induction process for e-vehicles. The authors built the model using the data and information provided in the reference papers and developed the initial stage-1 model. The power factor is improved by 0.1764 units. The applied model gives the good power factor without any boost converter is found to be 0.8545, with cuk converter is 0.9312 and with boost converter is 0.99. However, the power factor is improved by 0.1259 units. Hence, the efficiency of the overall system is improved significantly by using the boost converter rather than a cuk converter. Because of the development of this enhanced model, we can conclude that boost converter provides 505 units such that 40.11% better power factor

REFERENCES

[1] J. K. Nama, A. K. Verma, M. Srivastava, and P. S. Tomar, "An Efficient Inductive Power Transfer Topology for Electric Vehicle Battery Charging," IEEE Transaction on Industry Applications, vol. 56, no. 6, November/December 2020.

[2] M. Al-Saadi, A. Al-Omari, S. Al-Chlaihawi, A. Al-Gizi, and A. Crăciunescu, "Inductive Power Transfer for Charging the Electric Vehicle Batteries", in Electrotehnica, Electronica, Automatica (EEA), vol. 66, no.4, pp.29-39, ISSN 1582-5175, 2018.

[3] M. Bharathidasan and V. Indragandhi, "Review of Power Factor Correction (PFC) AC/DC-DC Power Electronic Converters for Electric Vehicle Applications," IOP Conf. Ser.: Mater. Sci. Eng. 906 012006, 2020.

[4] Y. Han, H. Xu, D. Li, Z. Zhang, "Research of the Single-Switch Active Power Factor Correction for the Electric Vehicle Charging System", International Conference on Electronic Engineering and Computer Science, IERI Procedia 4, pp. 126-132, 2013.

[5] A. Mahesh, B. Chokkalingam, and L. Mihet-Popa, "Inductive Wireless Power Transfer Charging for Electric Vehicles-A Review", IEEE Access, vol. 9, pp. 137667-137713, October, 2021.

[6] G. R. Kalra, B. S. Riar, and D. J. Thrimawithana, “An Integrated Boost Active Bridge Based Secondary Inductive Power Transfer Converter”, IEEE Transactions on Power Electronics, vol. 35, no. 12, December 2020

[7] H. Jafari, M. Moghaddami, T. O. Olowu, A. I. Sarwat, and M. Maryam, “Virtual Inertia-Based Multipower Level Controller for Inductive Electric Vehicle Charging Systems,” IEEE Journal Of Emerging And Selected Topics In Power Electronics, Vol. 9, No. 6, December 2021.

[8] S. Jayalath, and A. Khan, “Design, Challenges, and Trends of Inductive Power Transfer Couplers for Electric Vehicles: A Review,” IEEE Journal of Emerging and Selected Topics In Power Electronics, vol. 9, no. 5, October 2021.

[9] D. Wang, X. Qu, Y. Yao, and P.Yang, “Hybrid Inductive-Power- Transfer Battery Chargers for Electric Vehicle Onboard Charging With Configurable Charging Profile,” IEEE Transactions On Intelligent Transportation Systems, Vol. 22, No. 1, January 2021.

[10] P. Machura , V. D. Santis, and Q. Li, “Driving Range of Electric Vehicles Charged by Wireless Power Transfer” IEEE Transactions of Vehicular Technology, vo. 69, no. 6, June 2020.

[11] K. Onai, and J. O. Ojo, “Performance Analysis and Design of Frequency Controlled Series-Series Compensated Inductive Power Transfer System for Electric Vehicle Battery Charging,” IEEE Transactions on Industry Applications, vol. 58, no. 1, January/February 2022.

[12] G. R. Kalra, D. J. Thrimawithana, B. S. Riar, C. Huang, and M. Neuburger, “A Novel Boost Active Bridge-Based Inductive Power Transfer System,” IEEE Transactions on Industrial Electronics, vol. 67, no. 2, February 2020.

[13] X. Wang, J. Xu, S. Lu, S. Ren, M. Leng, and H. Ma, “Single-Receiver Multioutput Inductive Power Transfer System with Independent Regulation and Unity Power Factor,” IEEE Transactions on Power Electronics, Vol. 37, No. 1, January 2022.

[14] H. Zhang, Y. Chen, C. Jo, S. Park, D. Kim, “DC-Link and Switched Capacitor Control for Varying Coupling Conditions in Inductive Power Transfer System for Unmanned Aerial Vehicles,” IEEE Transactions on Power Electronics, Vol. 36, No. 5, May 2021.

[15] J. Zhou, P. Yao, Y. Chen, K. Guo, S. Hu, and H. Sun, “Design Considerations for a Self-Latching Coupling Structure of Inductive Power Transfer for Autonomous Underwater Vehicle,” IEEE Transactions on Industry Applications, Vol. 57, No. 1, January/February 2021.

[16] M. Singh, O. Singh, and A. Singh, "Renewable Energy Sources Integration in Microgrid including Load Patterns", 3rd IEEE International Conference on Recent Developments in Control, Automation & Power Engineering, RDCAPE-2019.

[17] S. Ann, and B. K. Lee, “Analysis of Impedance Tuning Control and Synchronous Switching Technique for a Semi-bridgeless Active Rectifier in Inductive Power Transfer Systems for Electric Vehicles,” IEEE Transactions On Power Electronics, Vol. 36, No. 8, August 2021